Catalysis of the Retinal Subpicosecond Photoisomerization Process in Acid Purple Bacteriorhodopsin and Some Bacteriorhodopsin Mutants by Chloride Ions

S. L. Logunov,* M. A. El-Sayed,* and J. K. Lanyi#
*School of Chemistry and Biochemistry, Georgia Institute of Technology, Atlanta, Georgia 30332, and #Department of Physiology and Biophysics, University of California, Irvine, Irvine, California, USA

ABSTRACT The dynamics and the spectra of the excited state of the retinal in bacteriorhodopsin (bR) and its K-intermediate at pH 0 was compared with that of bR and halorhodopsin at pH 6.5. The quantum yield of photoisomerization in acid purple bR was estimated to be at least 0.5. The change of pH from 6.5 to 2 causes a shift of the absorption maximum from 568 to 600 nm (acid blue bR) and decreases the rate of photoisomerization. A further decrease in pH from 2 to 0 shifts the absorption maximum back to 575 nm when HCl is used (acid purple bR). We found that the rate of photoisomerization increases when the pH decreases from 2 to 0. The effect of chloride anions on the dynamics of the retinal photoisomerization of acid bR (pH 2 and 0) and some mutants (D85N, D212N, and R82Q) was also studied. The addition of 1 M HCl (to make acid purple bR, pH 0) or 1 M NaCl to acid blue bR (pH 2) was found to catalyze the rate of the retinal photoisomerization process. Similarly, the addition of 1 M NaCl to the solution of some bR mutants that have a reduced rate of retinal photoisomerization (D85N, D212N, and R82Q) was found to catalyze the rate of their retinal photoisomerization process up to the value observed in wild-type bR. These results are explained by proposing that the bound Cl^- compensates for the loss of the negative charges of the COO^- groups of Asp85 and/or Asp212 either by neutralization at low pH or by residue replacement in D85N and D212N mutants.

INTRODUCTION

Bacteriorhodopsin, a retinal protein present in the membrane of *Halobacterium salinarium* (Oesterhelt and Stoeckenius, 1971), functions as a light-driven proton pump that establishes a proton gradient across the cell membrane. Proton translocation occurs during the photochemical cycle (Lozier et al., 1975), initiated by the absorption of a photon:

$$\mathrm{bR} \xrightarrow{0.5\ \mathrm{ps}} \mathrm{J} \xrightarrow{3\ \mathrm{ps}} \mathrm{K} \xrightarrow{1.5\ \mu\mathrm{s}} \mathrm{L} \xrightarrow[-\mathrm{H}^+]{50\ \mu\mathrm{s}} \mathrm{M} \xrightarrow[+\mathrm{H}^+]{\mathrm{ms}} \mathrm{N} \rightarrow \mathrm{O} \rightarrow \mathrm{bR}$$

The light-adapted bR contains all-*trans* retinal. Femtosecond studies of light-adapted bR have shown that subsequent to the absorption of a photon, 13-*cis* retinal (J) is formed in approximately 0.5 ps from the excited state (Pollard et al., 1986; Mathies et al., 1988; Dobler et al., 1988). J decays in 3 ps to the relatively long-lived intermediate K (Nuss et al., 1985). K decays to L in 1.5 μs, and the protonated Schiff base (PSB) loses its proton to form the M intermediate in 50 μs. As a result, a proton is released to the extracellular surface of the membrane. The reprotonation of the Schiff base takes place in the M $\rightarrow$ N process, when a proton is translocated from the cytoplasmic side, thus creating the transmembrane proton gradient. Retinal reisomerization from 13-*cis* to all-*trans* occurs in the N $\rightarrow$ O process. The protein relaxes to its original conformation in the O $\rightarrow$ bR process (Popp et al., 1993; Lanyi, 1993).

The retinal absorption shows a large opsin shift (5100 cm^{-1} at neutral pH) (Honig et al., 1976) in bR, which is responsible for its characteristic purple color. Absorption maximum is at λ_{max} = 568 nm in light-adapted bR. There are numerous investigations of the opsin shift origin (Honig et al., 1976; Nakanishi et al., 1980; Bagley et al., 1982; Harbison et al., 1983). It is currently thought to be due to a combination of various chromophore-protein interactions (Lugtenburg et al., 1986).

Another opsin effect is the protein catalysis of the primary process of retinal photoisomerization. The rate of photoisomerization of retinal increases from a few ps^{-1} in solution (Kandori et al., 1992) to $(0.5\ ps)^{-1}$ in bR (Nuss et al., 1985; Pollard et al., 1986; Mathies et al., 1988). Equally important is the fact that the photoisomerization becomes highly specific around the C13-C14 bond in bR, whereas in solution it occurs around several bonds (Koyama et al., 1991; Freedman and Becker, 1986). These opsin effects were discussed in terms of stabilization of a positive charge on C13 in the excited state by the nearby negatively charged Asp85 (Song et al., 1993). This changes the C13=C14 double-bond order present in the ground state into single-bond order in the excited state, and thus reduces the barrier for photoisomerization. This, together with steric effects either between the retinal methyl groups and the amino acid residues or resulting from the interaction between an anisotropic charge distribution of the protein around the retinal and the charge distribution in the retinal excited state (Xu et al., 1996), makes the photoisomerization extremely rapid.

Received for publication 17 January 1996 and in final form 22 May 1996.
Address reprint requests to Dr. Moustafa A. El-Sayed, Department of Chemistry and Biochemistry, Georgia Institute of Technology, Atlanta, GA 30332. Tel.: 404-894-0292; Fax: 404-894-0294; E-mail: mostafa.el-sayed@chemistry.gatech.edu.

0006-3495/96/09/1545/09 $2.00

Recent spectroscopic studies of site-specific mutants suggest that Asp-85, Asp-212, Arg-82, and Glu-204 are involved in the proton release from the Schiff base to the cytoplasmic side, whereas Asp-96 serves as proton donor during the subsequent protonation of the Schiff base from the cytoplasmic side (Marti et al., 1991; Oesterhelt et al., 1989; Needleman et al., 1991; Brown, 1995). In the proposed structural model of bR (Henderson et al., 1990) the carboxylate side chains of Asp-85 and Asp-212 are located approximately equidistant (4 Å) from the PSB. Mutagenesis experiments have shown that either one of Asp-85 and Asp-212 ionized residues can function as a counter-ion for the PSB (Khorana et al., 1991). However, neutral replacement of the Asp-85 has a greater effect on the proton pump function of bR than D212 (Marti et al., 1991). FTIR studies (Fahmy et al., 1993) suggest that Asp85 is the proton acceptor for the PSB in the L→M process.

It was also shown that removal of metal cations or acidification considerably affects the absorption maximum of the chromophore (Figher and Oesterhelt, 1979). This eliminates the deprotonation of the PSB and changes the retinal excited state dynamics (Kobayashi et al., 1990). When cations are removed, the absorption maximum shifts to the red (λ_{max} = 600 nm) to give deionized blue bR. At the same time the decay of the retinal excited state becomes biexponential with an average lifetime of 9 ps, which is 18 times longer than that for bR at pH 6.5 (Song et al., 1993; Logunov et al., 1996). Similar effects are observed when the pH of the solution is decreased to 2 (Kobayashi, 1990). At pH 2, D85N is protonated (Metz et al., 1992). It was also shown that the replacement of the charged residues Asp-85, Asp-212, or Arg-82 with neutral ones greatly affects the position of the chromophore's absorption maximum (Needleman et al., 1991), as well as its excited state decay (Song et al., 1993; Logunov et al., 1996). It was concluded (Song et al., 1993) that both the lifetime of the excited state and the shape of absorption spectrum are sensitive to the distribution of the charged groups within the retinal cavity.

Further acidification of bR at pH 0 shifts the retinal absorption maximum back to that for wild bR (λ_{max} = 565 nm at pH 0, HCl solution) to give acid purple bR. It was shown (Mowery et al., 1979) that this shift is more sensitive to the nature of the negative ion than to the pH value. The use of H_2SO_4, for example, has less effect on the absorption maximum than HCl at the same pH. The most interesting feature of bR at pH 0 is the possibility that it might pump Cl^- anion across the membrane (Der et al., 1991), which makes it similar to another natural pigment-protein complex, halorhodopsin. The addition of salt to the mutants D212N, D85N also affects the chromophore spectrum, suggesting that external anions can interact electrostatically with the PSB (Marti et al., 1992). In halorhodopsin, a light-driven chloride ion pump that is the equivalent of Asp85 is threonine. Recently it was shown that the replacement of Asp85 by threonine in bacteriorhodopsin converts it to a chloride ion pump (Sasaki et al., 1995).

In the present paper we report on the effect of decreasing the pH from 2 to 0 and the addition of salts on the rate of the chromophore photoisomerization in wild-type bR and in D212N, D85N, and R82Q mutants. We compare the results with those for halorhodopsin. The longest lifetime of the excited state for bR was found to be at pH 2 and for D85N mutant. All studied perturbations of bR at pH 2 cause acceleration of the photoisomerization rate. The data show that the addition of 1 M NaCl at pH 2 has a catalysis effect on the excited-state lifetime similar to that of decreasing the pH value from 2 by the addition of HCl. Furthermore, the addition of 1 M NaCl to the mutants with a reduced rate of retinal photoisomerization is found to catalyze their rates. The strong effect of the addition of chloride anions on the dynamics of retinal photoisomerization is discussed in terms of the previously proposed valence bond description of the excited state wave function of retinal and the changes in the charge distribution within the retinal cavity by the different perturbations (Song at al., 1993; Logunov et al., 1996).

MATERIALS AND METHODS

Bacteriorhodopsin cells were grown from the master slants of *Halobacterium solinarium* ET1-001 strain (kindly provided by Prof. Bogomolni at UC Santa Cruz). The purple membrane was isolated and purified as described previously (Needleman et al., 1991). The gel of bR was prepared according to the method of Mowery et al. (1979) for the measurement at pH lower than 2. All samples were light adapted for at least 30 min, and the measurements were completed at room temperature unless otherwise specified.

The laser system and transient spectroscopy set-up were described previously (Logunov et al., 1994, 1996). Briefly, the laser system consists of a commercial Coherent Satory dye laser pumped by an Antares mode-locked YAG laser. The resulting 250-fs pulses with a repetition rate of 80 MHz at wavelengths between 595 and 605 nm were amplified by a regenerative amplifier (Quantel, RGA 60) in a dye amplifier (Quantel, PTA 60) at 10 Hz. An amplified pulse with an energy of 1 mJ and 400 fs pulse duration was obtained. The optical density of the samples used in the transient absorbance measurements was about 1.0 at the excitation wavelength. The excitation wavelength was chosen to be 605 nm for the transient absorption experiment and 595 nm for photoacoustic measurements. The transient spectra were measured in the wavelength range 420–750 nm.

Photoacoustic measurements were completed as described previously (Logunov et al., 1996). The laser beam, with diameter D, was fixed by use of a pinhole of 0.2 mm size. This gives an effective acoustic transit time in water of 135 ns. The sample cuvette was attached to the surface of the transient transducer (Panametrics, V101-RM) and to Peltier elements for the temperature control. To improve the signal-to-noise ratio, all photoacoustic signals were amplified 100 times and stored in a transient digitizer (LeCroy 9450). The signal handling was similar to that described previously (Schulenberg et al., 1994).

A solution of $CoCl_2$ with absorbance of 0.2 at the wavelength of excitation (595 nm) was used as a calorimetric reference. The sample suspension was stirred after every 100 shots. The optical density of acid purple bR was adjusted to 0.2 at the excitation wavelength. The use of the calorimetric reference $CoCl_2$ eliminates the geometrical factors and the sensitivity of the transducer. Under these conditions the ratio of the slopes of photoacoustic signal versus I_{exc} (laser intensity) for the sample and for the reference gives the fraction of the heat that promptly dissipates in the sample. In addition to the volume change due to heating, conformational changes, specially for large biological molecules, can induce a pressure

wave. We examined these effects in a manner similar to that described previously (Schulenberg et al., 1994).

RESULTS

Acid purple bR

Transient spectroscopy

The absorption maximum of bR at pH 0 in 1 M HCl solution is at λ = 565 nm. Absorption difference spectra obtained after excitation by a 400-fs laser pulse are shown in Fig. 1. The bleach of the ground state at 570 nm and the excited-state absorption at 480 nm are observed immediately after the laser excitation. The decay of the excited state could be fitted to a biexponential decay with lifetimes of 0.8 and 7 ps (Fig. 2 *B*) and amplitude ratio of 0.6:1.0 (Table 1). The recovery of absorption at 570 nm (Fig. 2 *D*) reflects the ground-state recovery, which is due to the nonradiative decay from the excited-state, ground-state vibrational relaxation, and formation of J- and K-like intermediates. The lifetime of the fast component of the absorption change recovery at 570 nm correlates well with the fast component lifetime of the excited-state decay and probably is due to the ground-state recovery from the excited state. The long-lived component of absorption changes at 570 nm, which is represented as offset in the time scale of our experiment, reflecting the completion of the J- to K-intermediate transition time. The intermediate component, with a lifetime of 4 ps, may be assigned to the K-intermediate formation time or to vibrational relaxation of the hot ground state.

The transient difference spectrum in the 610–680-nm region recorded after a 20-ps delay corresponds to what is expected from the absorption of the K intermediate. The rise time of this intermediate is derived from the kinetics observed at 570 nm and was found to be about 4 ps. The transient spectra and kinetics of bR at pH 6.5 in gel were also measured for comparison (Fig. 2, *A* and *C*). The decay of the excited state was found to be close to that of bR in solution and was equal to 0.5 ps.

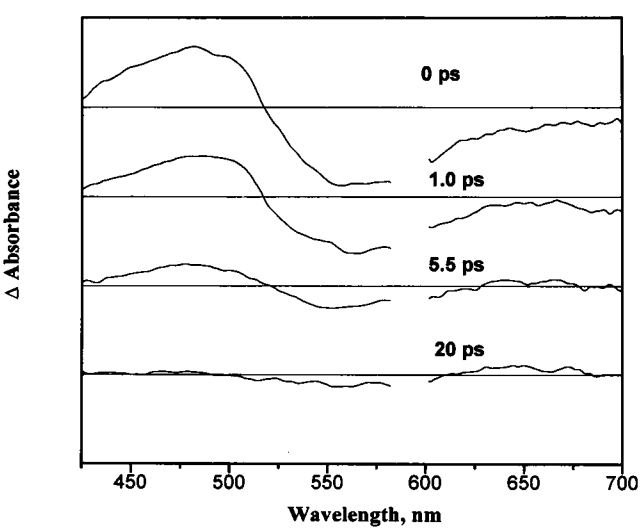

FIGURE 1 The transient absorption data for the bR gel at pH = 0 (1 M HCl). The spectra were taken at times zero, 1.0, 5.5, and 20 ps after excitation with a 400-fs, 600-nm laser pulse.

Photoacoustic study

Photoacoustics data provide an estimation of the quantum yield of photoisomerization and energy content in the K-intermediate. As was shown previously (Rohr et al., 1992; Logunov et al., 1996), the energy balance equation may be written as

$$1 - \alpha = \Phi E_K / E_{ph}, \quad (1)$$

where E_{ph} is absorbed photon energy, Φ is the quantum yield of photoisomerization, E_K is the energy of the K-intermediate relative to the bR ground state, and α is the amount of heat given off by the sample after photoexcitation. We have assumed here that 1) the quantum yield of the K intermediate formation is equal to the quantum yield of L intermediate and therefore of the photocycle ($\Phi_K = \Phi_L = \Phi$); 2) the quantum yield of fluorescence is negligible, and 3) the integration time of 130 ns is considerably shorter than the lifetime of the K-intermediate.

The plots of the photoacoustic signal versus laser power for acid purple bR and the reference ($CoCl_2$) with matched absorbance are shown in Fig. 3. Generally, the amplitude of the photoacoustic signal can be expressed as

$$H = B\alpha I_{exc}(1-10^{-A}) \quad (2)$$

where I_{exc} is the laser intensity; A is the absorbance of the sample; B is the proportionality factor reflecting geometrical factor, solvent parameters, and thermoelastic properties of the media; α is a fraction of the absorbed energy dissipated to the solvent as heat. Use of the reference compound, which dissipates all energy absorbed to the solvent, helps to eliminate geometrical factor B. From the ratio of the slopes of the straight lines given in Fig. 3 (between the observed amplitude of the photoacoustic signal (H) and laser intensity (I_{exc}); Eq. 2), the parameter H_S/H_R is determined, where H_S and H_R are the amplitudes of photoacoustic signals for the sample and reference.

As was proposed by Schulenberg et al., the photoacoustic signal has two components: one is due to the thermal expansion, and the other is due to the conformational changes in the protein. These two terms can be separated by measurements of H_S/H_R at different temperatures. Because thermal expansion of water is small at temperatures close to 4°C, the measurements of the photoacoustic signal at low temperatures will eliminate the contribution of the first term. As shown previously (Schulenberg et al., 1994), H_S/H_R could be expressed as

$$H_S/H_R = \alpha + \Delta V_R \Phi c_p \rho / (\beta E_{ph}), \quad (3)$$

where c_p, ρ, and β are the heat capacity at constant pressure, and the density and the thermal expansion of water, respec-

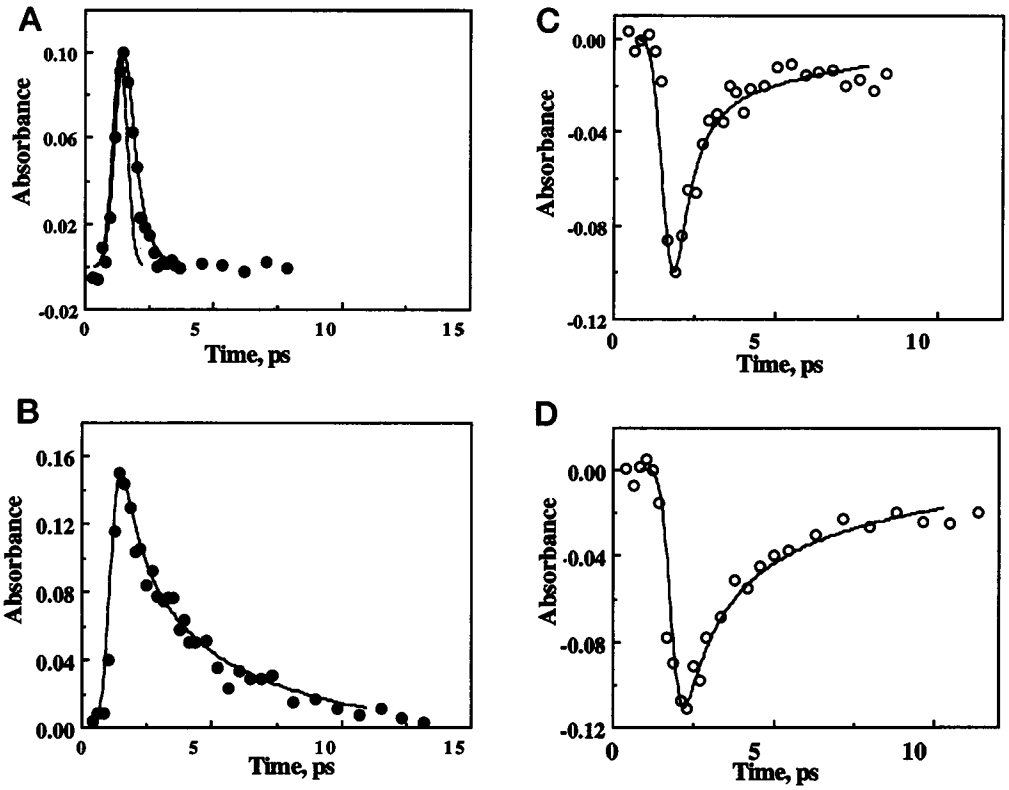

FIGURE 2 The kinetic profile of exited state absorption of retinal in gel sample of native bR at pH 6.5, 480 nm (*A*) and of acid purple bR at pH 0, 480 nm (*B*); and the ground-state bleach recovery at 570 nm of native bR at pH 6.5 (*C*) and of acid purple bR at pH 0 (*D*). The solid lines are best fit with parameters shown in Table 1.

tively. Φ is the quantum yield of photoisomerization, ΔV_R is the volume changes of bR during K intermediate formation, and E_{ph} is the energy of the exciting photon. The dependence of H_S/H_R on $c_p\rho/\beta$ is shown in the inset of Fig. 3. The thermal expansion of water has strong temperature dependence. Thus, to change parameter $c_p\rho/\beta$, it is enough to change the temperature. The plot shown in Fig. 3 was measured in the temperature range of 10–30°C. The parameter β is also very sensitive to the concentration of the ions in the water. Because the extinction coefficient of the $CoCl_2$ is low at 595 nm, its concentration in the solution had to be high. In the temperature dependence experiments we used malachite green dye as reference and adjusted the ionic strength of the solution with NaCl to match the ionic strength of a 1 M HCl (pH 0) solution. The plot of H_S/H_R versus $c_p\rho/(\beta E_{ph})$ should be linear. The intercept gives the value of α, and the slope corresponds to the volume changes due to conformational contribution. It is evident that this slope is very flat, indicating that the contribution to the photoacoustic signal due to conformational changes is small. We estimated this change to be -3 ± 1 cm^3/mol. Under more physiological conditions (pH 6.5) a similar

TABLE 1 The kinetic data for the excited-state decay (470–480 nm) and ground-state recovery (580 nm)

Sample	τ_1 (ps)	τ_2 (ps)	A1	A2	A3
bR gel, pH 6.5 (480 nm)	0.5	5	0.95	0.02	—
bR, pH 2, 480 nm	2.0	17.0	0.5	0.5	—
bR gel, pH 0, 480 nm	0.8	7.0	0.37	0.63	—
bR gel, pH 0, 570 nm	0.8	4.0	0.4	0.52	0.08
bR gel, pH 2, 1 M NaCl, 480 n	1.5	8.0	0.45	0.55	—
bR gel, pH 2, 1 M NaCl, 580 n	1.2	8.0	0.6	0.3	0.1
bR gel, pH 0, H_2SO_4, 480 nm	2.0	20.0	0.63	0.37	—
bR gel, pH 0, H_2SO_4	2.0	20.0	0.6	0.33	0.07
D212N, pH 4.5, 480 nm	2.0	6.0	0.6	0.4	—
D212N, 1 M NaCl, 480 nm	1.0	—	1.0	—	—
D212N, 1 M NaCl, 580 nm	1.0	4.0	0.74	0.15	0.11
D85N, pH 4.5, 480 nm	2.0	12.0	0.45	0.55	—
D85N, 2 M NaCl, 480 nm	0.5	10.0	0.55	0.45	—
D85N, 2 M NaCl, 580 nm	0.5	5.0	0.5	0.4	0.1
R82Q, pH 5.0, 480 nm	1.6	7.0	0.75	0.25	—
R82Q, 1 M NaCl, 480 nm	1.6	7.0	0.87	0.13	—
R82Q, 2 M NaCl, 580 nm	1.3	7.0	0.9	0.05	0.05

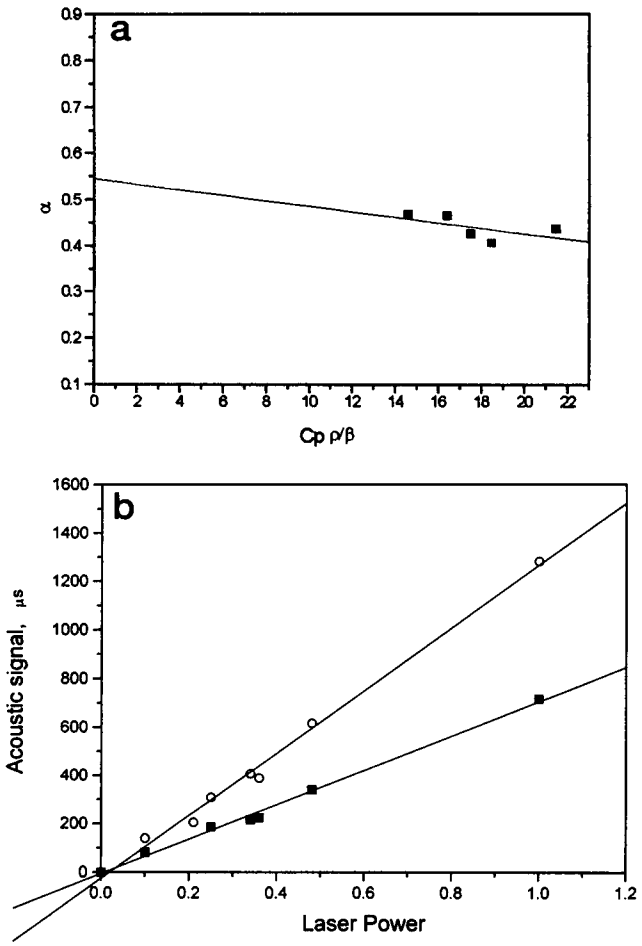

FIGURE 3 Plot of the photoacoustic signal intensity versus laser power of the reference compound (cobalt chloride, ○) and solution of bR at pH 0 (■). The laser pulse duration is 400 fs, heat integration time is 130 ns. The amount of the stored heat could be determined from the ratio of the slopes. (*Inset*) Dependence of the ratio H_S/H_R versus $c_p\rho/\beta$. Intercept of the linear fit corresponds to the α (see Eq. 2).

contraction was observed with normal bR (-11 cm^3/mol by Shulenberg et al., 1994, and -7.8 ± 3 cm^3/mol by Tsuda and Ebrey, 1980).

Equation 1 contains two unknown parameters, Φ and E_K. From the photoacoustic experimental data one can estimate the lower limit for the quantum yield of photoisomerization to be 0.5, by assuming that the maximum value of E_K is equal to the energy of the 0–0 band of the bR molecules (i.e., when all electronic excitation of the retinal is stored in the K- intermediate). Assuming the quantum yield is unity, we obtain, in turn, 105 kJ/mol for the lower limit for the energy content in the K intermediate.

We used the estimated lower limit of 0.5 for the quantum yield of isomerization to fit the observed spectrum of the K-intermediate in the few tens of picoseconds time domain. The total number of photoexcited bR molecules was obtained by deconvolution of the transient spectrum at zero time in the region 500–650 nm to two components: the excited-state absorption and ground-state bleach. The number of the bR molecules that participate in the photocycle was obtained by deconvolution of the transient spectrum at a delay time of 20 ps from the absorption spectrum of the K-intermediate absorption spectrum and ground-state bleach. The ratio of the two numbers gives the quantum yield of photoisomerization (0.6). The excited state and K-intermediate absorption spectra obtained in the deconvolution procedure are shown in Fig. 4. Because of strong overlap of the K-intermediate and ground-state absorption spectra, the error for the quantum yield value was determined to be 20%.

Low pH or anion effects on the rate of photoisomerization

We used H_2SO_4 to make acidic bR to study the effect of anions on the dynamics of photoisomerization. It is known (Mowery et al., 1979) that the absorption maximum of bR at pH 2 in a solution of H_2SO_4 is the same as that in HCl. At pH 0 the absorption maximum in H_2SO_4 solution is at 595 nm, which is red shifted from that in HCl solution by 30 nm. Mower et al. suggested that the nature of the negative ion is important for this blue-purple transition. The dynamics of the excited state at pH 0 in the case of H_2SO_4 was found to be biexponential with lifetimes of 2.0 and 20.0 ps, with an amplitude ratio of 1:0.6 (Table 1). These two components may originate from the mixture of all-*trans* and 13-*cis* isomers or from some other heterogeneity of the sample. The fast component in the excited-state decay corresponds to the photoisomerization of all-*trans* retinal isomer, as was suggested previously (Logunov et al., 1996). The slow component is due to other retinal isomers. We used the average lifetime of the excited state and lifetimes of the fast and slow component to compare dynamics of photoisomerization in different samples. The average lifetime was cal-

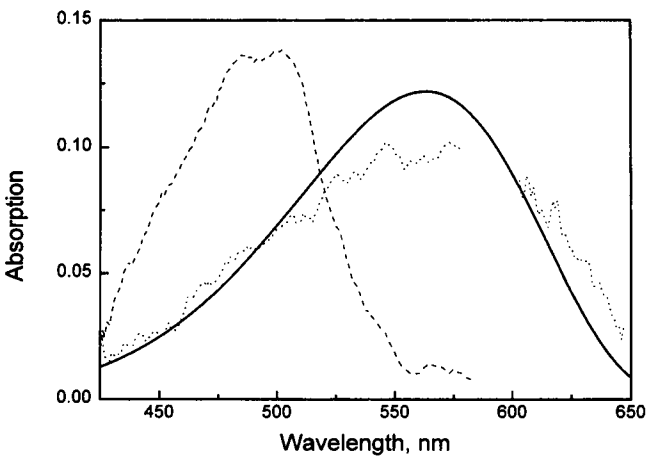

FIGURE 4 The deconvolution of the spectra, shown in Fig. 1 (time zero, and 20 ps), to the ground state bleaching (solid curve in the middle), excited state absorption (dashed line on the left), and K intermediate absorption (dotted curve at the right), assuming a quantum yield of isomerization equal to 0.6.

culated as $\tau_{av} = \Sigma A_i \tau_i$, where τ_i is the lifetime and A_i is the relative amplitude of component i. The average lifetime when using H_2SO_4 to adjust the pH to 0 was found to be 8.7 ps, and the fast and slow component lifetimes were 2.0 and 20.0 ps, respectively. This is close to the average lifetime and lifetimes of the fast and slow components of the excited state at pH 2 (9.5, 2.0, and 17.0 ps, respectively), but double the value observed at pH 0 when using HCl (4.5, 0.8, and 7.0 ps, respectively). Thus, the nature of the anion also affects the dynamics of the retinal photoisomerization at pH 0.

Chloride ion effect on the rate of photoisomerization

At pH 2 the absorption maximum of retinal in bR is at 600 nm. At pH 2 with 1 M NaCl, bR maximum absorbance is at 575 nm, which is red shifted from the absorption maximum at pH 0 (565 nm). The decay of the excited state at pH 2 with 1 M of NaCl is biexponential, with lifetimes of 1.5 and 8 ps and with an amplitude ratio of 1:1.2 (Table 1). The average lifetime of the excited state under these conditions is 5.05 ps, which is close to the average lifetime of bR at pH 0. This may indicate that 1 M NaCl at pH 2 has the same effect on the dynamics of the photoisomerization as does the lowering of pH from 2 to 0 by using HCl.

The acceleration (catalytic) effect of Cl^- on the retinal photoisomerization process is defined as the ratio of its rate (measured by $1/\tau$, where τ is the excited state lifetime) with Cl^- to that without. The effect on acid blue bR is determined by adding HCl or NaCl. The effect on mutants is determined by the effect of adding NaCl to mutant solutions at pH 4.5–5. The results are shown in Table 2.

The absorption maximum of D85N at pH 4.5 is at 605 nm. The excited-state decay is biexponential with lifetimes of 1.5 and 12 ps, and an amplitude ratio of 1:1.2 (Table 1). Upon the addition of 2 M NaCl, the absorption maximum shifts to 585 nm. The excited-state dynamics becomes faster than that at low NaCl concentration, and the decay was found to be biexponential with lifetimes of 0.5 and 10.0 ps and an amplitude ratio of 1:1. The acceleration factor is 1.54 (Table 2).

In the R82Q mutant, the absorption maximum at pH 4.5 is at 595 nm. Asp-85 is largely protonated under these conditions (Brown et al., 1993). The addition of 1 M of NaCl causes a shift of the absorption maximum to 585 nm. The data for the excited state lifetimes and relative amplitudes under these condition are given in Table 1. The acceleration factor is found to be 1.28 (Table 2), which is less than that for D85N and acid blue bR.

In the D212N mutant, the charged aspartate residue is replaced with the neutral asparagine. This mutant has absorption maximum at 565 nm at pH 4.5. The excited state of this mutant under these conditions decays biexponentialy with lifetimes of 2.0 and 6.0 ps and an amplitude ratio of 3:2. The average lifetime of the excited state is 3.6 ps. The addition of 1 M NaCl does not have any significant effect on the absorption maximum (562 nm), but the dynamics of photoisomerization becomes considerably faster. The decay of the excited state was found to be monoexponential, with a lifetime of 1.0 ps (Fig. 5). The acceleration factor was found to be 3.6. The acceleration factors for the different samples are given in Table 2.

For comparison we also calculated the acceleration factor based on the lifetime of the fast and slow components. These two components correspond to the all-*trans* configuration retinal and other isomers, respectively. This is given in Table 2. There is a clear correlation between acceleration factors obtained from the calculation of the average lifetimes and lifetimes of photoisomerization for all-*trans* iso-

TABLE 2 The lifetimes of the excited state (fast, slow component, and average) and "acceleration factor" calculated based on the fast, slow component lifetimes, and average lifetime of the excited-state decay after the addition of a high concentration of chloride ions

Sample	Photoisomerization lifetime (ps)			Acceleration factor			Absorption maximum (nm)
	Fast	Slow	Avg.	Fast	Slow	Avg.	
Effect on acid blue bR							
pH 6.5	0.5	5.0	0.5	—	—	—	568
pH 2.0	2.0	17.0	9.5	—	—	—	600
pH 2.0 + 1 M NaCl	1.5	8.0	5.05	1.3	1.88	1.88	565
pH 0 HCl	0.8	7.0	4.5	2.5	2.1	2.1	575
pH 0 H_2SO_4	2.0	20.0	8.7	1.0	0.85	1.09	595
Effect on mutants							
D212N, pH 4.5	2.0	6.0	3.6	—	—	—	565
D212N, pH 4.5, 1 M NaCl	1.0	1.0	1.0	2.0	6.0	3.6	562
D85N, pH 4.5	2.0	12.0	7.9	—	—	—	605
D85N, pH 4.5, 2 M NaCl	0.5	10.0	4.6	4.0	1.2	1.54	585
R82Q, pH 4.5	1.6	7.0	2.95	—	—	—	595
R82Q, pH 4.5, 2 M NaCl	1.6	7.0	2.3	1.0	1.0	1.28	585

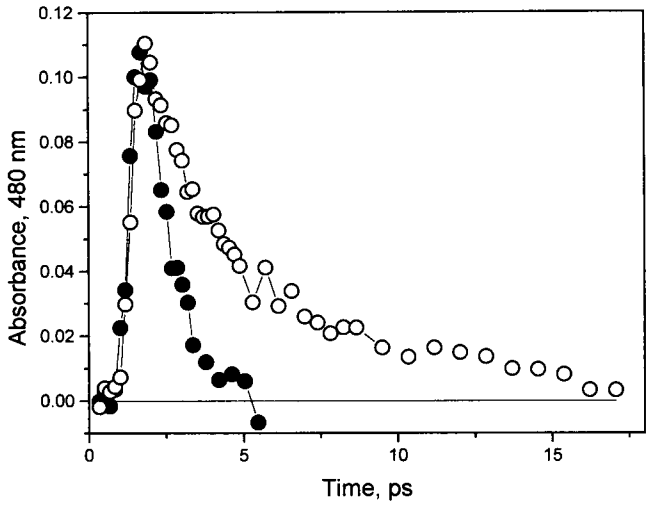

FIGURE 5 The kinetic of the excited-state decay, measured at 480 nm, for mutant D212N at pH 4.5 (○), and the same sample after the addition of 1 M NaCl (●).

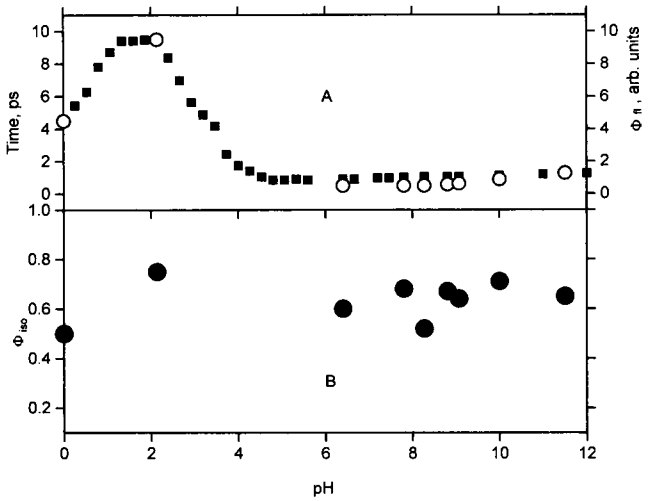

FIGURE 6 The dependence of the fluorescence quantum yield on the pH (■, taken from Kouyama et al., 1985), the average lifetime of the excited state (○) measured in this paper (pH 0 and pH 2) together with our data measured previously (Logunov et al., 1994) (*A*), and quantum yield of the retinal photoisomerization (triangles), measured in this paper and previously (Logunov et al., 1994, 1996) (*B*).

mer and other retinal isomers. The best correlation among these three acceleration factors is found for the chloride ion effect on acid blue bR. There is some difference in acceleration factors calculated for the fast and slow components' lifetime, and the average lifetime for D212N and D85N mutants.

DISCUSSION

Acid purple bR has an average excited-state lifetime of 4.5 ps. This value of average lifetime of the excited state at different pHs correlates well with the fluorescence quantum yield data (Kouyama et al., 1985) (Fig. 6). In Fig. 6 the quantum yield of fluorescence (Kouyama et al., 1985) is plotted together with the average lifetime of the excited state measured in this and earlier papers (Logunov et al., 1994, 1996). Good correlation is observed for the pH ranging from 0 to 11. A comparison of the excited-state lifetimes shows that the average lifetime of the excited state of acid purple bR is twice as long as that for halorhodopsin (Kandori et al., 1992). The shape of the excited-state absorption of acid purple bR is very similar to that of bR at pH 6.5 (Logunov at al., 1996), but it is narrower and blue shifted by 30 nm when compared to that of halorhodopsin. Our estimate shows that the quantum yield of photoisomerization in acid purple bR is 0.6 ± 0.12, which is higher than that for halorhodopsin (0.3; Kandori et al., 1992; Oesterhelt et al., 1985) and close to that of bR at pH 6.5. The spectrum of the K intermediate is close to that of bR at pH 6.5 but is lower in extinction coefficient (Fig. 4).

Previous studies of the spectroscopic properties of the double mutant D85N/D212N expressed in *Escherichia coli* suggested that the anion replaces protonated Schiff base counter-ions by binding directly to the Schiff base (Marti et al., 1992). However, the exact locations of the chloride anions are not clear. The lifetime of the excited state, as shown previously (Song et al., 1995; Logunov et al., 1996), is sensitive to the charge distribution around a C13=C14 double bond. The photoisomerization lifetime was found to increase by a factor of 2 as pH was changed from 2 to 0 by using HCl. The average lifetime of the excited state of bR at pH 2 with 1 M NaCl is close to that of bR at pH 0. This suggests that the negatively charged Cl^- anion might be in a similar position in these acid purple bR and bR at pH 2 with 1 M NaCl. The photoisomerization dynamics in bR at pH 0 (1 M HCl), bR at pH 2 with 1 M NaCl, and D85N at pH 4.5 with the addition of 2 M NaCl are all similar. In acid bR as well as in D85N, the aspartate 85 is changed to neutral residue. This "poisons" the catalysis of the retinal photoisomerization by the negative charge of the aspartate group (Song et al., 1993). The addition of Cl^- could then replace the negatively charged aspartate 85, and thus recover the protein catalysis for the photoisomerization process.

In mutants D85N and D212N the acceleration factors calculated from the lifetimes of the fast and slow components in the excited-state decay were found to be somewhat different. These mutants consist of a mixture of all-*trans* and 13-*cis* isomers because of their fast dark adaptation time (Song et al., 1995). The fast component corresponds to the photoisomerization of all-*trans* retinal, and the slow component to the 13-*cis* isomer. The difference in acceleration factors for these two isomers of retinal suggests that chloride ions have different access to the C13 double bond for different isomers. In the case of D85N the largest acceleration was found for all-*trans* isomer (4.0), whereas in D212N the strongest effect was found for 13-*cis* retinal (6.0).

Mutant D212N shows a normal photocycle in the presence of chloride ion (Ref. 15 in Sasaki et al., 1995). This is apparently due to the anion replacing D212 as the Schiff base counter-ion. In this system, bR still transports protons rather than chloride ions, because of the fact that in this mutant, D85, the proton acceptor remains intact. The large acceleration effect of NaCl found in D212N (3.6, average lifetimes of D212N excited state are 3.6 ps at pH 4.5 and 1.0 ps with 1 M NaCl added) supports this observation. This suggests that the chlorine anions supply the negative charges lost by neutral residue replacement of aspartates 85 and 212. The fact that the catalysis by Cl^- does not decrease the photoisomerization lifetime by the same amount as the COO^- of the aspartate group suggests that they are not located at exactly the same position with respect to the C13 of the retinal. Thus, their stabilization for the positive charge on this atom in the excited states is not equally effective.

CONCLUSION

A catalytic effect of chloride anion was shown for retinal photoisomerization in bacteriorhodopsin when its rate is perturbed by lowering the pH or by site-directed mutagenesis. These results are explained by the compensation of the lost negative charge of the COO^- group of Asp85 (either by neutralization or by residue replacement) by the chloride anion.

The authors thank Mr. Temer S. Ahamdi for his help in the preparation of the manuscript.

We thank the Department of Energy, Office of Basic Energy Sciences (grant DE-FG03-88ER-13828), for financial support.

REFERENCES

Albech, A., N. Friedman, M. Shaves, and M. Ottolenghi. 1989. Factor affecting the absorption maxima of acidic forms of bacteriorhodopsin. *Biophys. J.* 56:1259–1265.

Anot, B., A. G. Douches, R. H. Callender, B. Becher, and T. Ebrey. 1977. Resonance Raman studies of the purple membrane. *Biochemistry.* 16: 2995–2999.

Bagchi, B., and G. Fleming. 1990. Dynamics of activationless reaction in solution. *J. Phys. Chem.* 94:9–20.

Bagley, K., G. Dollinger, L. Eisenstein, K. Singh, and L. Zimanyl. 1982. Fourier transform infrared difference spectroscopy of bacteriorhodopsin and its products. *Proc. Natl. Acad. Sci. USA.* 79:4972–4976.

Braslavky, S. E., and G. E. Heibel. 1992. Time-resolved photothermal and photoacoustic methods applied to photoinduced processes in solution. *Chem. Rev.* 92:1381–1410.

Brown, L. S. 1995. *J. Biol. Chem.* 270:27122–27126.

Brown, L. S., L. Bonet, R. Needleman, and J. K. Lanyi. 1993. Estimated asid disslocation canstants of the Schiff base, Asp-85, and Arg-85 during the bacteriorhodopsin photocycle. *Biophys. J.* 65:124–130.

Der, A., S. Szaraz, R. Toth-Boconadi, Z. Tokayi, L. Keszthelyi, and W. Stoeckeneus. 1991. Alternative translocation of protons and halide ions by bacteriorhodopsin. *Proc. Natl. Acad. Sci. USA.* 88:4751–4755.

Dobler, J., W. Zinth, W. Laiser, and D. Oesterhelt. 1988. Excited state reaction dynamics of bacteriorhodopsin studied by femtosecond spectroscopy. *Chem. Phys. Lett.* 144:215–220.

Fahmy, K., O. Weidlich, M. Engelhard, H. Sigrist, and F. Siebert. 1993. Aspartic acid-212 of bacteriorhodopsin is ionized in the M and N photocycle intermediates: an FTIR study on specifically ^{13}C-labeled reconstituted purple membrane. *Biochemistry.* 32:5862–5868.

Figher, U., and D. Oesterhelt. 1979. Chromophore equilibration in bacteriorhodopsin. *Biophys. J.* 28:211–230.

Freedman, K. A., and R. S. Becker. 1986. Comparative inverstigation of the photoisomerization of the protonated and unprotonated *n*-butylamine Schiff bases of 9-*cis*, 11-*cis*, 13-*cis* and all-*trans*-retinals. *J. Am. Chem. Soc.* 108:1245–1251.

Harbison, G. S., J. Herzfeld, and R. C. Griffin. 1983. Solid-state nitrogen-15 nuclear magnetic resonance study of the Schiff base in bacteriorhodopsin. *Biochemistry.* 22:1–5.

Henderson, R., J. M. Baldwin, T. A. Ceska, F. Zemin, E. Beckman, and K. H. Dowing. 1990. Model for structure of bacteriorhodopsin based on high resolution electron cryomicroscopy. *J. Mol. Biol.* 213:899–929.

Honig, B., A. D. Greenbarg, U. Dimer, and T. G. Ebrey. 1976. Visual-pigment spectra: implication of the protonation of the retinal schiff base. *Biochemistry.* 15:4593–4599.

Kandori, H., K. Yoshihara, H. Tomioka, and H. Sasabe. 1992. Primary photochemical events in halorhodopsin studied by subpicosecond time-resolved spectroscopy. *J. Phys. Chem.* 96:6066–6071.

Kobayashi, T., M. Terauchi, T. Kouyama, M. Yoshizawa, and M. Taiji. 1990. Femtosecond spectroscopy of acidified and neutral bacteriorhodopsin. *SPIE Laser Appl. Life Sci.* 1403:407–416.

Kouyama, T., K. Kinosita, Jr., and A. Ikegami. 1985. Excited-state dynamics of bacteriorhodopsin. *Biophys. J.* 47:43–54.

Koyama, Y., K. Kubo, M. Komori, H. Yasuda, and Y. Mukai. 1991. Effect of protonation on the isomerization properties of *n*-butylamine Schiff base of isomeric retinal as revealed by direct HPLC analyses: selection of isomerization by retinal proteins. *Photochem. Photobiol.* 54:433–443.

Lanyi, J. K. 1993. Proton translocation mechanism and energetics of light-driven pump bacteriorhodopsin. *Biochim. Biophys. Acta.* 1183: 241–261.

Logunov, S. L., M. A. El-Sayed, L. Song, and J. K. Lanyi. 1996. Photoisomerization quantum yield and apparent energy content of the K-intermediate in the photocycles of bacteriorhodopsin, its mutants D85N, R82Q, D212N, and deionized blue bacteriorhodopsin. *J. Phys. Chem.* 100:2391–2398.

Logunov, S. L., L. Song, and M. A. El-Sayed. 1994. pH dependence of the rate and quantum yield of the retinal photoisomerization in bacteriorhodopsin. *J. Phys. Chem.* 98:10674–10677.

Lozier, R. H., R. A. Bogomolni, and W. Stoeckenius. 1975. Bacteriorhodopsin: a light-driven proton pump in *Halobacterium halobium. Biophys. J.* 15:955–963.

Lugtenburg, J., M. Muradin-Szweykowska, G. Heermans, J. A. Patdoen, G. S. Harbison, J. Herfeld, R. G. Griffin, S. O. Smith, and R. A. Mathies. 1986. Mechanism for the opsin shift of retinal's absorption in bacteriorhodopsin. *J. Am. Chem. Soc.* 108:3104–3105.

Marti, T., H. Otto, S. J. Rosselet, M. P. Heyn, and H. G. Khorana. 1992. Anion binding to the Schiff base of the bacteriorhodopsin mutants Asp85 → Asn/Asp-212 → Asn and Arg-82 → Gln/Asp-85 → Asn/Asp-212-Asn*. *J. Biol. Chem.* 267:16922–16927.

Marti, T., S. J. Rosselet, H. Otto, M. P. Heyn, and H. G. Khorana. 1991. The retinylidene Schiff base counterion in bacteriorhodopsin. *J. Biol. Chem.* 266:18674–18684.

Mathies, R. A., C. H. Brito Cruz, W. T. Pollard, and S. V. Schank. 1988. Direct observation of the femtosecond excited state *cis-trans* isomerization in bacteriorhodopsin. *Science.* 240:777–779.

Metz, G., F. Siebert, and M. Engelhard. 1992. Asp85 is the only internal aspartic acid that gets protonated in the M intermediate and the purple-to-blue transition of bacteriorhodopsin. A solid state ^{13}C CP-MAS NMR investigation. *FEBS Lett.* 303:237–241.

Mowery, P. C., R. H. Lozier, Q. Chae, Y.-W. Tsen, M. Taylor, and W. Stoeckenius. 1979. Effect of acid pH on the absorption spectra and photoreactions of bacteriorhodosin. *Biochemistry.* 18:4100–4107.

Nakanishi, K., V. Balogh-Nair, M. Arnaboldi, K. Tsujimobo, and B. Honig. 1980. An external point-charge model for bacteriorhodopsin to account for its purple color. *J. Am. Chem. Soc.* 102:7945–7947.

Needleman, R., M. Chang, B. Ni, G. Vago, J. Fornes, S. H. White, and J. K. Lanyi. 1991. Properties of Asp212-Asp bacteriorhodopsin suggest

that Asp212 and Asp 85 both participate in a counterion and proton acceptor complex near Schiff base. *J. Biol. Chem.* 266:11478–11484.

Nuss, M. C., Z. Zinth, W. Kaiser, E. Kolling, and D. Oesterhelt. 1985. Femtosecond spectroscopy of the first events of the photochemical cycle in bacteriorhodopsin. *Chem. Phys. Lett.* 117:1.

Oesterhelt, D., and W. Stoeckenius. 1971. Rhodopsin-like protein from the purple membrane of *Halobacterium halobium. Nature.* 233:149–152.

Polland, H.-J., F. Franz, W. Zinth, W. Kaizer, E. Kolling, and D. Oesterhelt. 1986. Early picosecond events in the photocycle of bacteriorhodopsin. *Biophys. J* 49:651.

Popp, A., M. Wolperdinger, N. Hampp, C. Branchle, and D. Oesterhelt. 1993. Photochemical conversion of the O-intermediate to 9-*cis*-retinal-containing products in bacteriorhodopsin films. *Biophys. J.* 65: 1449–1459.

Rohr, M., W. Gartner, G. Schweitzer, and S. E. Braslavky. 1992a. Quantum yield of the photochromic equilibrium between bacteriorhodopsin and its bathointermediate K. Femto- and nanosecond optoacoustic spectroscopy. *J. Phys. Chem.* 96:6055–6061.

Rohr, M., G. Schweitzer, W. Gartner, and S. E. Braslavky. 1992b. Detection of conformational changes during the photocycle of bacteriorhodopsin by laser induced optoacoustic spectroscopy (LIOAS). Structures and function of retinal proteins. Colloque INSERM. Vol. 221. J. L. Rigaud, editor. J. Libbey Eurotext Ltd. 151–154.

Sasaki, J., L. S. Brown, Y.-S. Chon, H. Kandori, A. Maeda, R. Needleman, and J. K. Lanyi. 1995. Conversion of bacteriorhodopsin into chloride pump. *Science.* 269:73–75.

Schulenberg, P. J., M. Rohr, W. Gather, and S. E. Braslavsky. 1994. Photoinduced volume changes associated with the early transformations of bacteriorhodopsin: a laser-induced optoacoustic study. *Biophys. J.* 66:838–843.

Song, L., M. A. El-Sayed, and J. K. Lanyi. 1993. Protein catalysis of the retinal subpicosecond photoisomerization in the primary process of bacteriorhodopsin photosynthesis. *Science.* 261:891–894.

Song, L., D. Yang, M. A. El-Sayed, and J. K. Lanyi. 1995. Retinal isomer composition in some bacteriorhodopsin mutants under light and dark adaptation conditions. *J. Phys. Chem.* 99:10052–10055.

Tittor, J., D. Oesterhelt, R. Maurer, H. Desel, and R. Uhl. 1987. The photochemical cycle of halorhodopsin absolute spectra of intermediates obtained by flash-photolysis and fast difference spectra measurements. *Biophys. J.* 52:999–1006.

Tsuda, M., and T. G. Ebrey. 1980. Effect of high pressure on the absorption spectrum and isomeric composition of *bR. Biophys. J.* 58:135–141.

Xu, D., C. Martin, and K. Schulten. 1996. Molecular dynamics study of early picosecond events in the bacteriorhodopsin photocycle: dielectric response, vibrational cooling and the J, K intermediates. *Biophys. J.* 70:453–460.